VOLUME 37 NUMBER 4
APRIL 2019

ISSN: 1002-0721
CODEN JREAE 6

Journal of Rare Earths

ELSEVIER

Project for Enhancing International Impact of China STM Journals

CONTENTS

SPECTROSCOPY, LUMINESCENCE AND PHOSPHORS

RARE EARTH CATALYSIS

MAGNETISM AND MAGNETIC MATERIALS

ADVANCED RARE EARTH MATERIALS

CHEMISTRY AND HYDROMETALLURGY

JOURNAL OF RARE EARTHS

Vol. 37 No. 4 (April 2019)

CONTENTS

SPECTROSCOPY, LUMINESCENCE AND PHOSPHORS

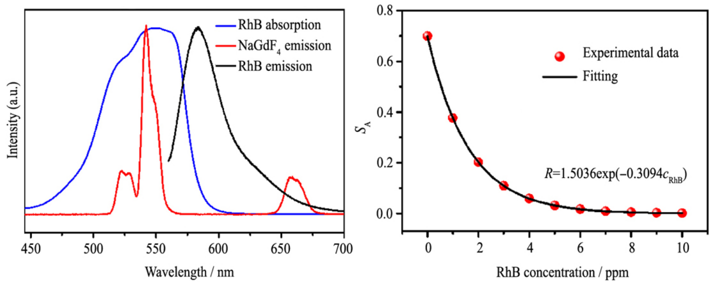

Hanping Xiong, Qiuhong Min, Hongqing Ma, Lei Zhao, Wenbo Chen, Jianbei Qiu, Xue Yu,Xuhui Xu

$NaGdF_4$:Yb^{3+},Er^{3+}@$NaGdF_4$ core-shell NPs exhibit strong green UC emission (520–569 nm) under the excitation of 980 nm laser when its shell thickness is 2.3 nm, which overlaps with the absorption band of RhB. Under the excitation of 545 nm laser, pure RhB emission peaks are observed at 585 nm. It indicates that the RhB molecules can absorb the green fluorescence emitted by Er^{3+} ions through the RET process. Based on this, a solid biosensor of $NaGdF_4$:Yb^{3+},Er^{3+}@$NaGdF_4$ NPs is used to detect RhB concentration, the maximum sensitivity 0.69959 ppm^{-1} is obtained at low RhB concentrations (<4 ppm). Thus, the ultra-high sensitivity detection by $NaGdF_4$:Yb^{3+},Er^{3+}@$NaGdF_4$ core-shell upconversion nanoparticles in low concentration can be realized

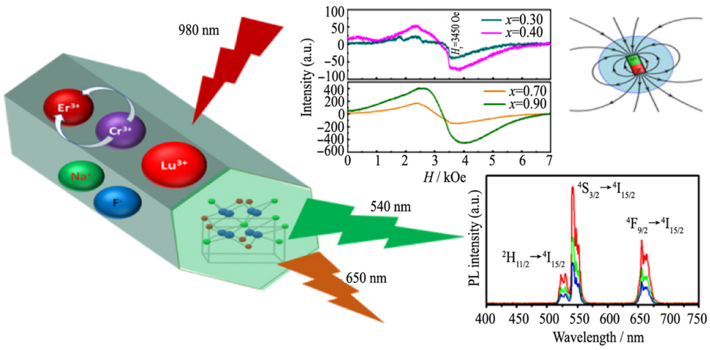

Bui The Huy, Zayakhuu Gerelkhuu, The-Long Phan, Ngo Tran, Yong-Ill Lee

Dual roles of Cr^{3+} ions in hexagonal phase of $NaLuCrF_4$:Er material

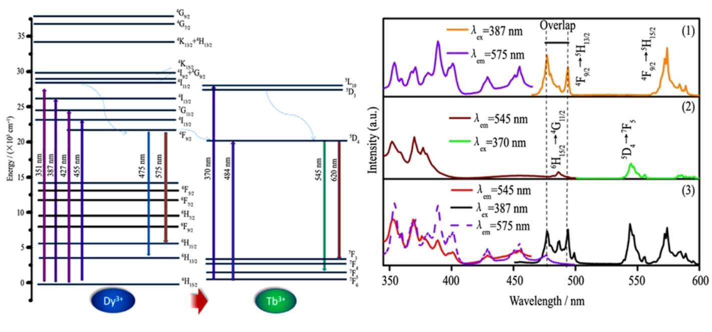

Yuanhong Liu, Yuan Xue, Ronghui Liu, Mingyue Chen, Guantong Chen, Chunpei Yan, Xia Zhang, Yu'nan Zhou, Wei Gao, Xiaole Ma

Energy transfer process from Dy^{3+} to Tb^{3+} in $La_3Si_6N_{11}$

356 Enhancement of luminescence intensity and spectroscopic analysis of Eu^{3+} activated and Li^{+} charge-compensated Bi_2O_3 nanophosphors for solid-state lighting

S. Ashwini, S.C. Prashantha, Ramachandra Naik, H. Nagabhushana

J. Rare Earths, (37) 2019: 356-364

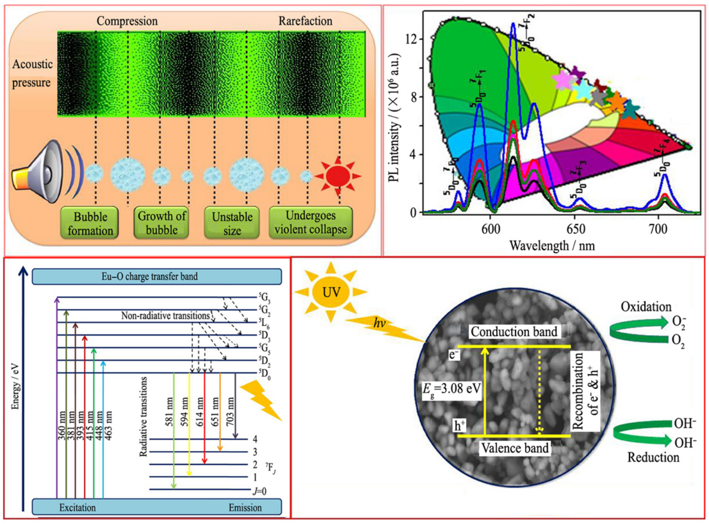

$Bi_2O_3:Eu^{3+},Li^{+}$ nanophosphors were prepared by sonication method. Morphology was tuned after adding EGCG. CIE diagram shows that nanophosphors emits red light. Li^{+} addition enhances emission intensity

365 Luminescence properties of near-UV excitable yellow-orange light emitting warm $CaSrAl_2SiO_7:Sm^{3+}$ phosphors

Shweta Sharma, Nameeta Brahme, D.P. Bisen, Pradeep Dewangan

J. Rare Earths, (37) 2019: 365-373

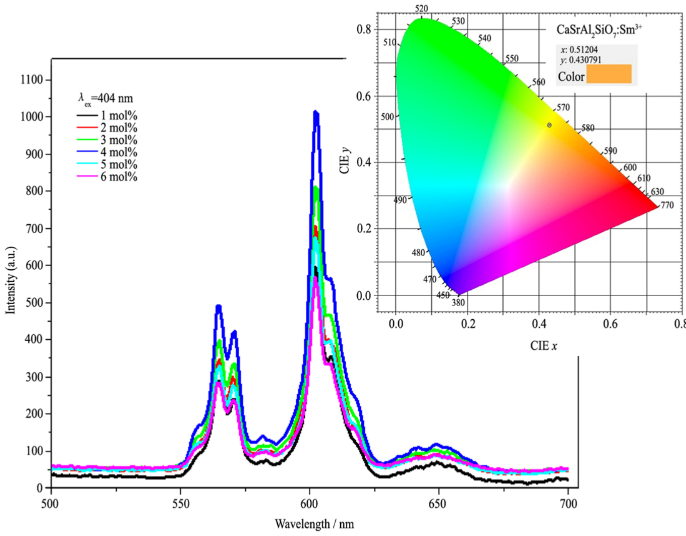

Sm^{3+} concentration dependent luminescence spectra of $CaSrAl_2SiO_7:Sm^{3+}$ phosphors observed in yellow-orange region and confirm suitability of the material for lighting application

374 Comparative study of Sm^{3+} ions doped phosphate based oxide and oxy-fluoride glasses for solid state lighting applications

M. Shoaib, G. Rooh, R. Rajaramakrishna, N. Chanthima, N. Kiwsakunkran, H.J. Kim, J. Kaewkhao, S. Tuscharoen

J. Rare Earths, (37) 2019: 374-382

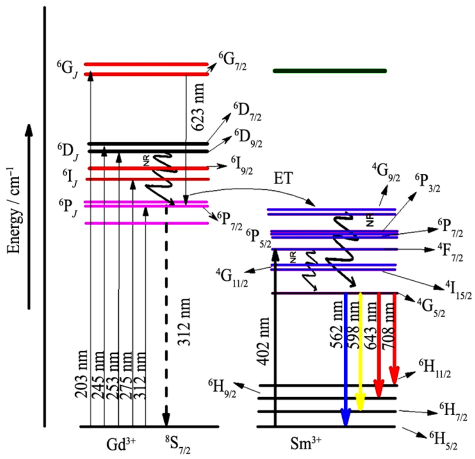

Energy level of Gd^{3+}/Sm^{3+} system

RARE EARTH CATALYSIS

383 Structure-activity relationship in water-gas shift reaction over gold catalysts supported on Y-doped ceria

Tatyana Tabakova, Lyuba Ilieva, Ivan Ivanov, Maela Manzoli, Rodolfo Zanella, Petya Petrova, Zbigniew Kaszkur

J. Rare Earths, (37) 2019: 383-392

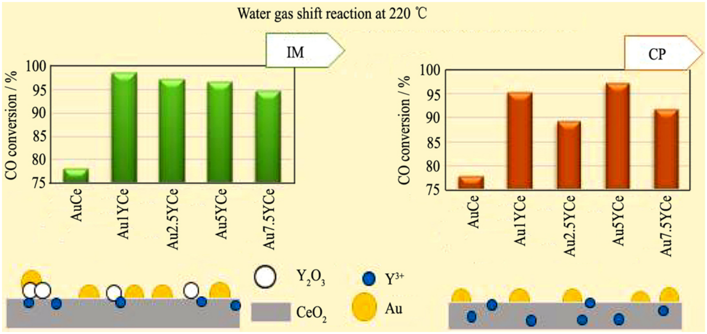

Water-gas shift activity of gold catalysts on Y-doped CeO_2 supports was studied.
Y-doped CeO_2 supports were prepared by impregnation and coprecipitation.
Effect of the Y_2O_3 amount as dopant on the WGS activity of Au/CeO_2 was examined.
Very high activity (> 90% CO conversion) in the range 180–220 °C was measured.
Effect of pre-treatment in air at 200 and 350 °C on WGS activity was studied

MAGNETISM AND MAGNETIC MATERIALS

393 Tailoring the mechanical anisotropy of sintered NdFeB magnets by Pr – Cu grain boundary reconstruction

Minghui Tang, Xiaoqian Bao, Xuejiao Zhang, Xing Mu, Kechao Lu, Jiheng Li, Xuexu Gao

J. Rare Earths, (37) 2019: 393-397

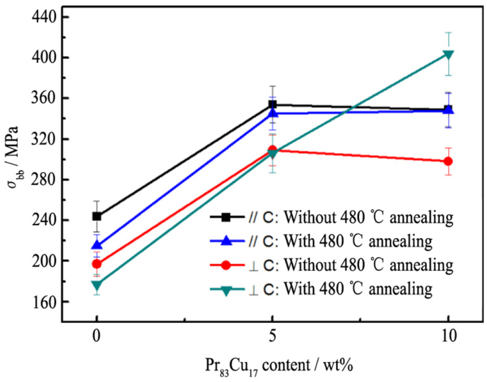

Bending strengths depend on $Pr_{83}Cu_{17}$ addition content and annealing process

398 Influence of Al/Cu content on grain boundary diffusion in Nd-Fe-B magnet via *in-situ* observation

Xinghua Cheng, Jian Li, Lei Zhou, Tao Liu, Xiaojun Yu, Bo Li

J. Rare Earths, (37) 2019: 398-403

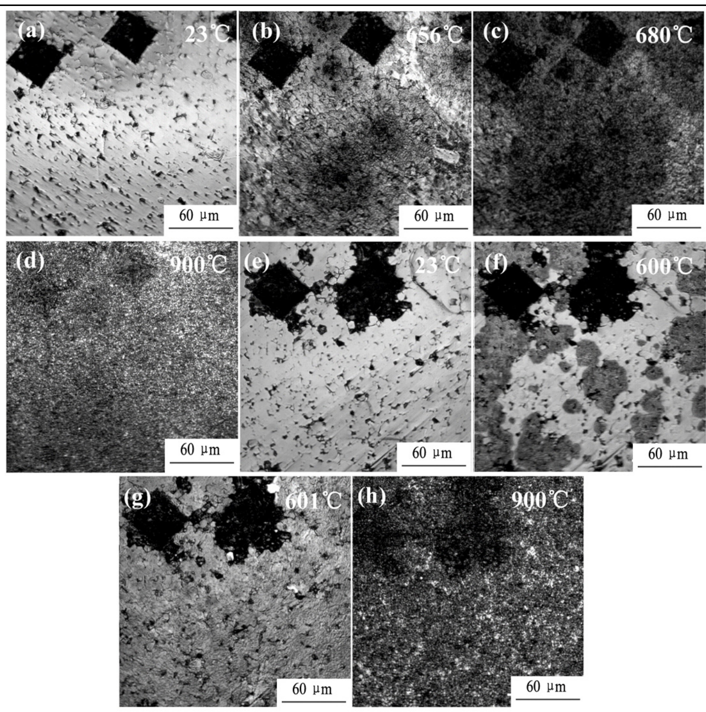

In order to further analyze the microstructural evolution during heating procedure, we utilized laser scanning confocal microscopy (LSCM) for *in-situ* observation, as shown in Fig. 5. The specimen with lower AlCu showed a slow expanding behavior of melting spots, while that with higher AlCu showed a flash expanding behavior. This is the direct evidence to prove that Al/Cu content plays a critical role in the melting of intergranular phase in Nd-Fe-B magnet

404 Tunable Curie temperature and magnetocaloric effect of FeCrMoCBYNi bulk metallic glass with different crystallized phases

Yuanbin Lv, Qingjun Chen, Youlin Huang

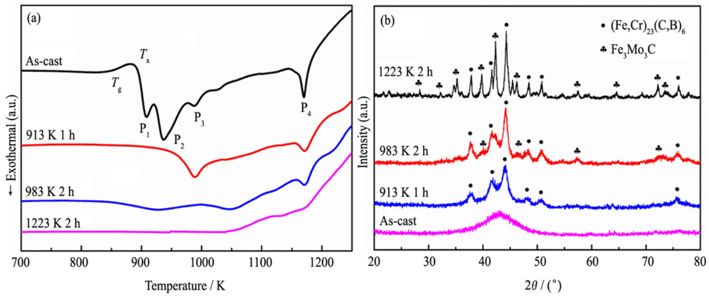

Different crystallized phases lead to different T_c in Fe-based samples. Different crystallized phases lead to different $\Delta S_M(T)$ in Fe-based samples. Multi-phase coexistence made Fe-based BMG reach an optimal value in $\Delta S_M(T)$

J. Rare Earths, (37) 2019: 404-409

ADVANCED RARE EARTH MATERIALS

410 Evolution of microstructures and optical properties of gadolinium oxide with oxygen flow rate and annealing temperature

Zhenhuai Yang, Lei Yang, Bing Dai, Pei Lei, Shuai Guo, Peng Wang, Qiang Wang, Yujie Ding, Yumin Zhang, Jiecai Han, Jiaqi Zhu

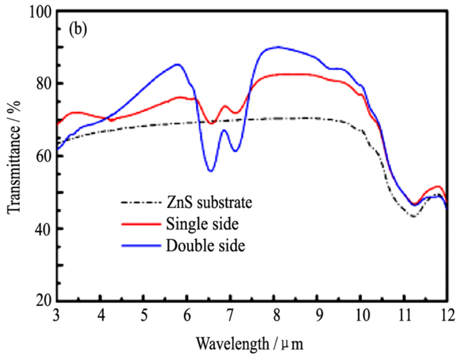

Gd_2O_3 films have potential application for anti-reflective coatings. The transmittance of ZnS substrate increased to about 90% at longer IR wavelengths range after double-sided coatings

J. Rare Earths, (37) 2019: 410-415

416 Enhancing optical absorption in visible light of ZnO co-doped with europium and promethium by first-principles study through modified Becke and Johnson potential scheme

A.G. El Hachimi, M.L. Ould NE, A. El Yousfi, A. Benyoussef, A. El Kenz

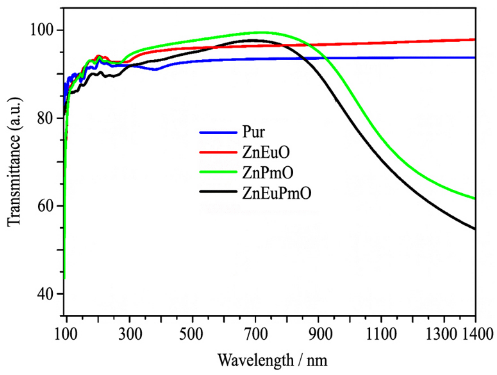

Transmittance for undoped ZnO, Eu atom doped ZnO, Pm atom doped ZnO and Eu, Pm co-doped ZnO

J. Rare Earths, (37) 2019: 416-421

422 Synergistic extraction of heavy rare earths by mixture of α-aminophosphonic acid HEHAMP and HEHEHP

Qi Zhao, Yanling Li, Shengting Kuang, Zhifeng Zhang, Xue Bian, Wuping Liao

J. Rare Earths, (37) 2019: 422-428

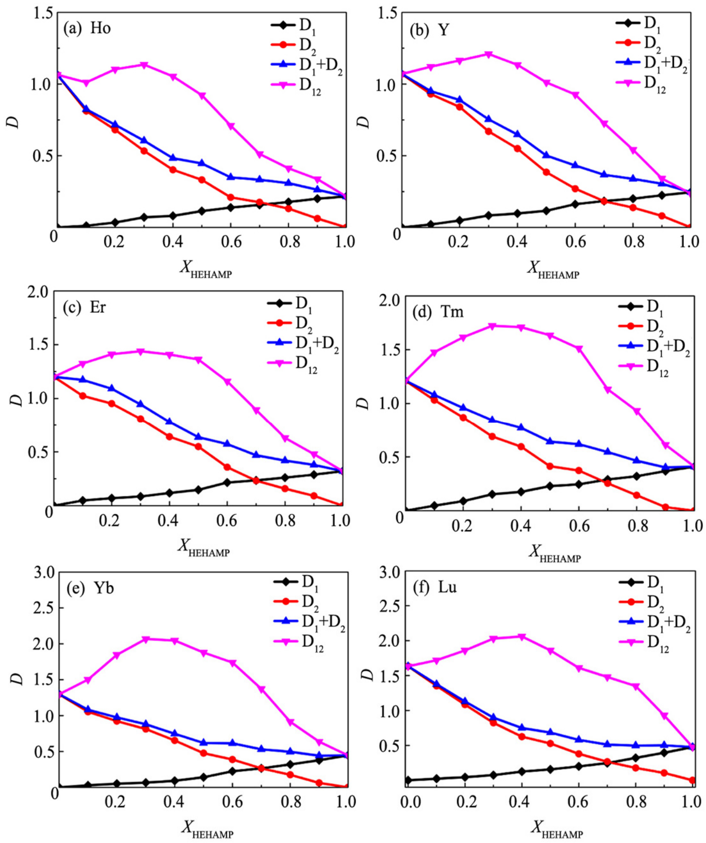

The mixtures of HEHAMP and HEHEHP show a remarkable synergistic effect on the extraction of REs

429 Leaching ion adsorption rare earth by aluminum sulfate for increasing efficiency and lowering the environmental impact

Lifen Yang, Cuicui Li, Dashan Wang, Fengyang Li, Yanzhu Liu, Xuezhen Zhou, Mingbiao Liu, Xiufeng Wang, Yongxiu Li

J. Rare Earths, (37) 2019: 429-436

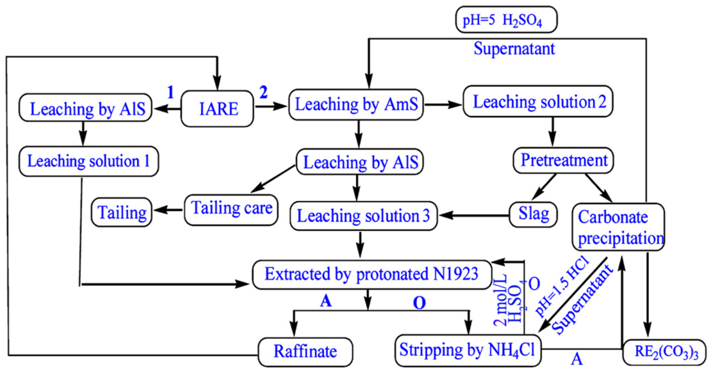

Novel procedures for leaching IARE using AlS as a leaching agent to increase the LE of IARE with lower waste water producing and landslide risk

437 Process optimization of neodymium chloride solutions precipitated by magnesium bicarbonate

Yannan Yan, Yang Xu, Xiaowei Huang, Zongyu Feng, Yongke Hou, Kai Li, Liangshi Wang, Yihanna Hu

J. Rare Earths, (37) 2019: 437-442

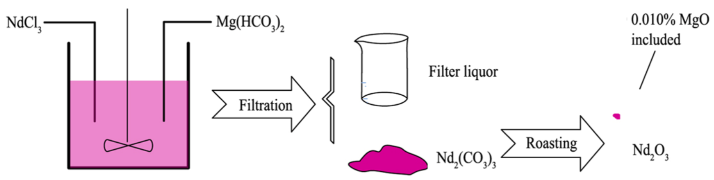

$NdCl_3$ and $Mg(HCO_3)_2$ were added into the tank reactor to produce $Nd_2(CO_3)_3$. The Nd_2O_3 was attained with 0.010% MgO after filtration and roasting

443 Separation and recovery of associated rare earths from the Zhijin phosphorite using hydrochloric acid

Dengpan Nie, An Xue, Mingyang Zhu, Yu Zhang, Jianxin Cao

J. Rare Earths, (37) 2019: 443-450

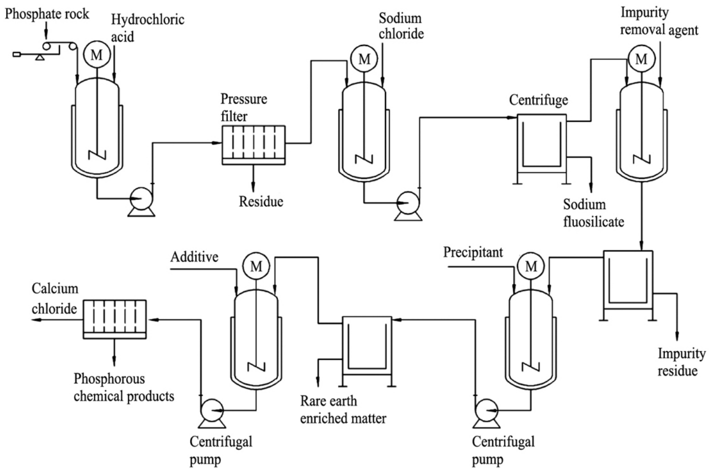

Hydrochloric acid was used to decompose phosphate rock. Defluorination, impurity removal, and multiple enrichment processes enabled the efficient separation and recovery of the phosphorite-associated rare earths from the acidolysis solution